Supplementary Information

Steric Hindrance Alleviation Strategy to Enhance the Photo Switching Efficiency of Azobenzene Functionalized Metal-Organic Framework Toward Tailorable Carbon Dioxide Capture

Qi Huang[a], Junju Mu[b], Zhen Zhan[d], Feng Wang[b*], Shangbin Jin[c*], Bien Tan[d*], Chunfei Wu[a*]

Materials Sythesis

Synthesis of ^{pazo}L and ^{mazo}L

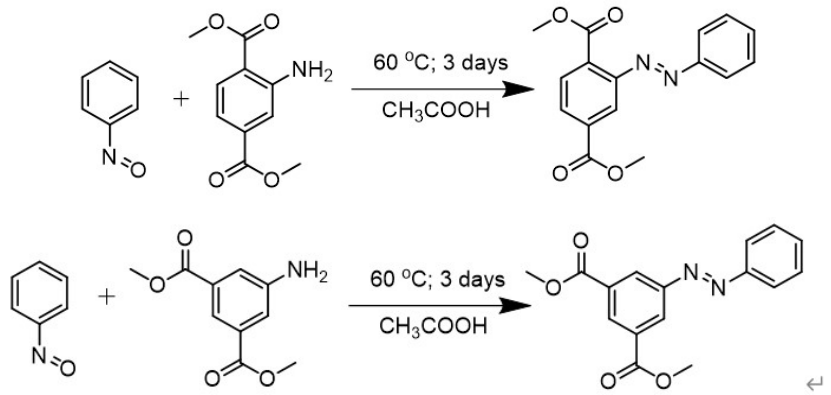

In a typical synthesis, 4.4 g (41 mmol) of nitrosobenzene and 4.2 (20 mmol) g of dimethyl aminoterephthalate/5-aminoisophthalate was dissolved in 180 mL of glacial acetic acid in a round bottom flask. The colour of the solution turned from dark green to dark brown and the solution was kept stirred for 3 days at 60 °C under reflux. The solution was then concentrated by evaporating the glacial acetic acid in a rotary evaporator and then neutralized using a saturated sodium hydrogen carbonate solution with stirring. The crude product was purified through column chromatography (from hexane : DCM : Et_2O = 8 : 1 : 1 to hexane : DCM : Et_2O = 4 : 1 : 1) to give dimethyl 2-(phenyldiazenyl)terephthalate (2.8 g, yield 46%), and dimethyl 5-(phenyldiazenyl)isophthalate. (3.0 g, yield 49%).^{1}H NMR of dimethyl 2-(phenyldiazenyl)terephthalate (400 MHz, DMSO-d_6) : δ 8.24 (d, 1H), 8.08 (q, 1H), δ 7.88 (m, 2H), δ 7.79 (d, 1H), and fδ 7.48 (m, 3H), δ 3.91 (s, 3H), δ 3.88 (s, 3H). ^{1}H NMR of dimethyl 5-(phenyldiazenyl)isophthalate (400 MHz, DMSO-d_6), δ (ppm): 8.74 (s, 1H); 8.70 (s, 2H); 7.90 (d, 2H); 7.50 (d, 3H), 3.90 (s, 6H).

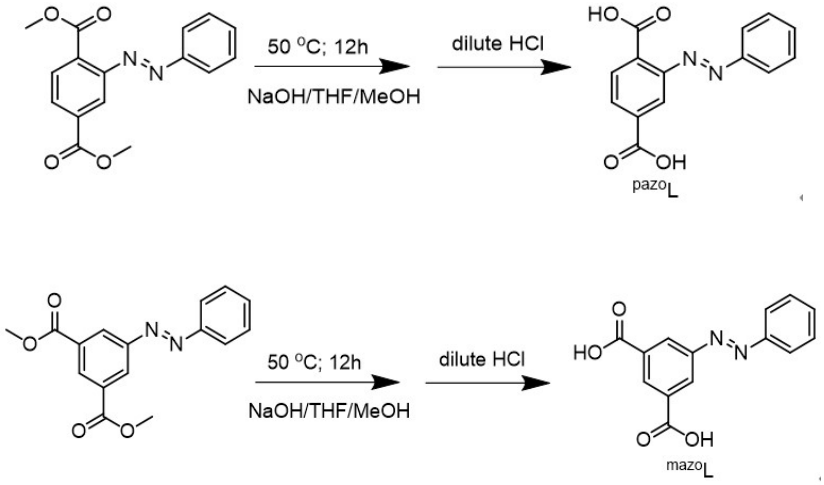

2.8 g of dimethyl 2-(phenyldiazenyl)terephthalate was then dissolved in a mixed solvent containing 20% NaOH, THF and methanol (1 : 1 : 1) at 50 °C for overnight. After stopping stirring and heating, there was obvious two separated organic and water phases in the system. The above organic phase was then removed while the aqueous part was acidified using 4 M HCl. While HCl solution dropped to the aqueous part, orange precipitation was soon formed. The orange precipitation obtained was back extracted using Et_2O. Finally, the Et_2O was evaporated to give orange solid, ^{pazo}L (2 g, yield 92%).^{1}H NMR (400 MHz, DMSO-d_6): δ 8.13 (q, 1H), δ 8.09 (d, 1H), δ 7.90 (q, 3H), δ 7.63 (m, 3H). Diethyl 5-(phenyldiazenyl)isophthalate (1.5 g, 5 mmol) was added to a 100 flask with THF, ethanol, 20% NaOH (15 ml/15 ml/15 ml) mixture, which was stirred overnight at 50 °C with reflux. After the organic phase was removed, 4 M HCl solution was added to obtain an orange precipitate. The orange precipitation obtained was back extracted using Et_2O. Finally, the Et_2O was evaporated to give orange solid, ^{mazo}L (1.2 g, yield: 92%).^{1}H NMR (400 MHz, DMSO-d_6), δ (ppm): 8.62 (s, 1H); 8.57 (s, 2H); 7.98 (d, 2H); 7.64 (d,3H).

DFT calculations

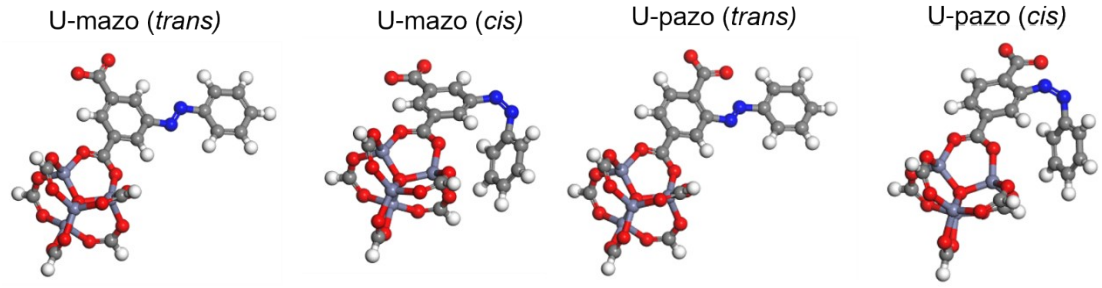

Figure S1. DFT-D2 optimized structures of U-mazo and U-pazo with azobenzene groups in trans and cis configurations. Color code for atoms: Zn, slate; C, gray; O, red; N, blue.

The Vienna Ab Initio Package (VASP)[1] was employed to perform spin-polarized DFT calculations within the generalized gradient approximation (GGA) using the PBE[2] functional formulation. The ionic cores were described by the projected

augmented wave (PAW) pseudopotentials[3] and valence electrons were explicitly taken into account using a plane wave basis set with energy cutoffs of 500 eV and 800 eV for structural optimization and total energy calculations, respectively. The Brillouin zone was sampled using a 1 × 1 × 1 and 3× 3 × 3 Γ-centered k-points mesh for structural optimization and total energy calculations, respectively. Partial occupancies of the Kohn−Sham orbitals were allowed using the Gaussian smearing method and a width of 0.05 eV. The electronic energy was considered self-consistent when the energy change was smaller than 10^{-6} eV. Geometry optimization was considered convergent when the ionic forces were less than 0.01 eV/Å. Grimme's DFT-D2 methodology[4] was used to describe the dispersion interactions among all the atoms.

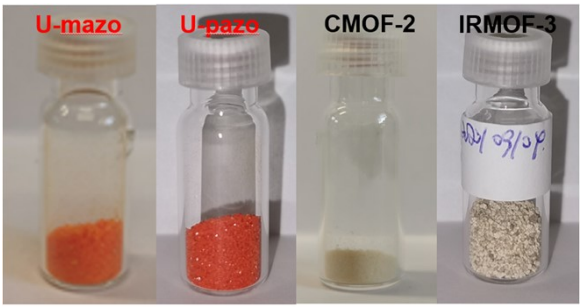

Figure S2. Pictures of MOF samples.

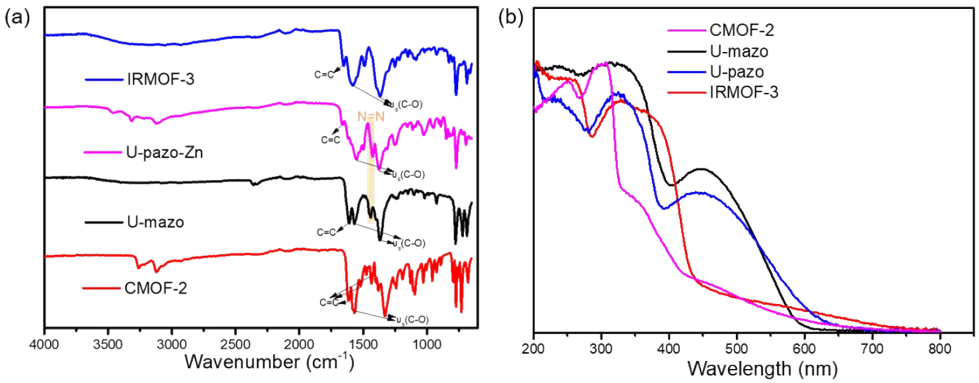

Figure S3. FT-IR spectra (a) and UV-visible light absorption spectra (b) of MOFs

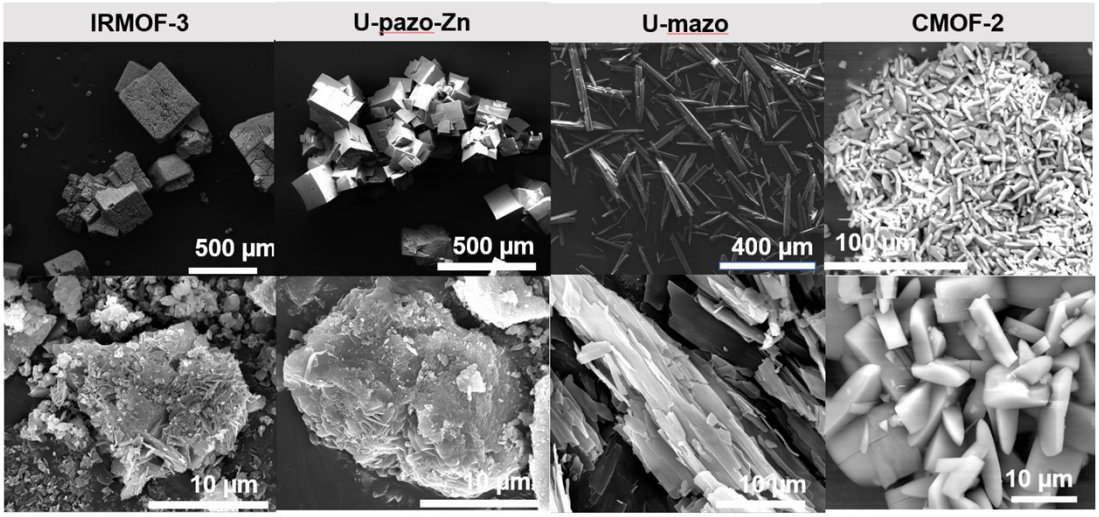

Figure S4. Scanning electron microscopy images of U-pazo, U-mazo, IRMOF-3 and CMOF-2.

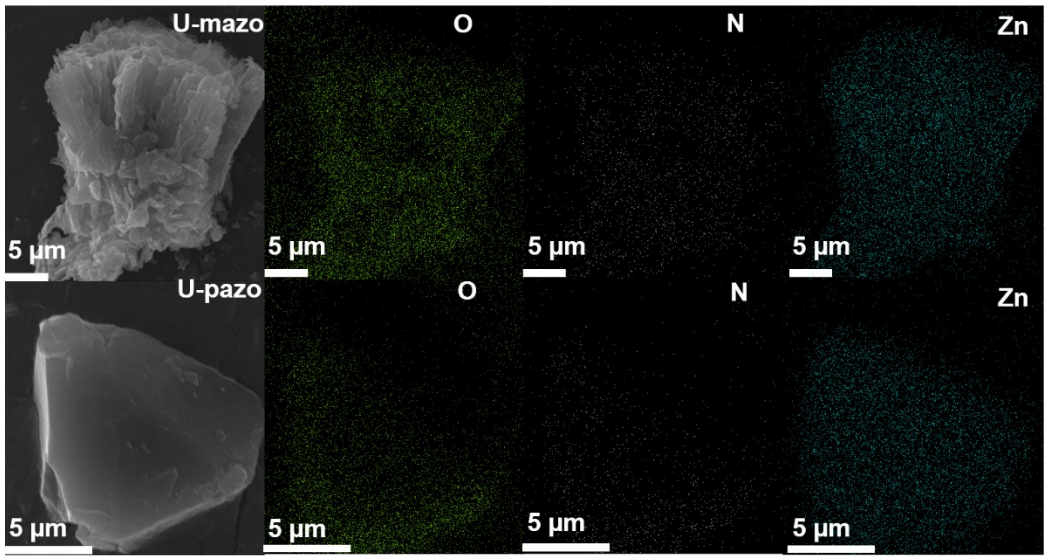

Figure S5. Scanning electron microscopy mapping images of U-mazo and U-pazo.

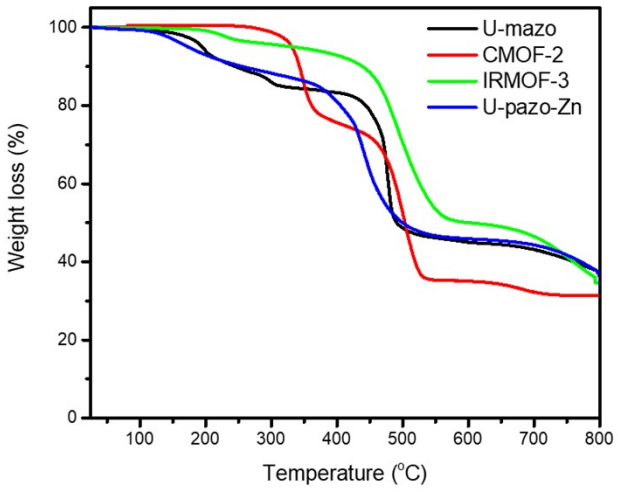

Figure S6. TGA curves of U-pazo, U-mazo, IRMOF-3 and CMOF-2.

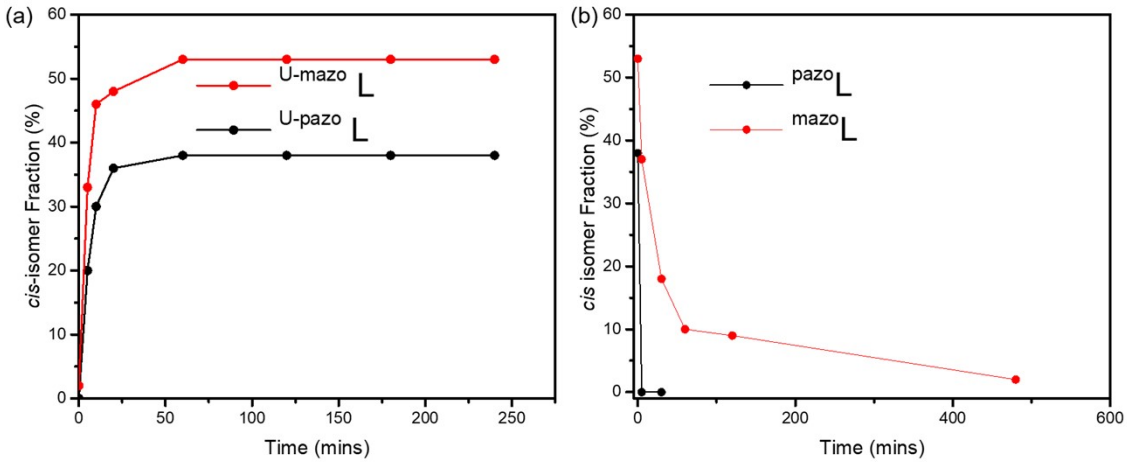

Figure S7. Changes in the cis-isomer content of ^{pazo}L and ^{mazo}L with time at 25 °C upon (a) irradiation with UV (365 nm) (b) and heating (80 °C), respectively.

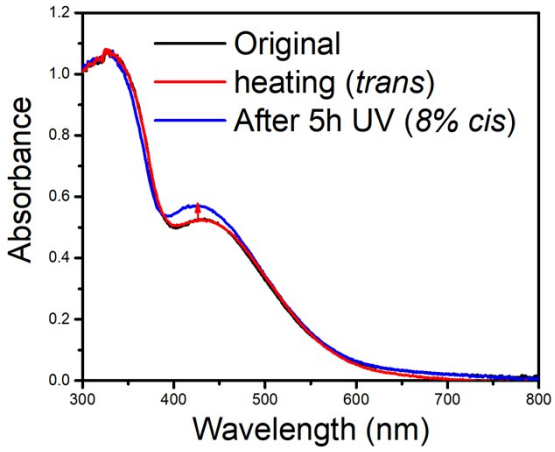

Figure S8. Diffuse reflectance spectra of U-pazo at 25 °C in the solid state upon irradiation with UV (365nm) and then heating at 80 °C.

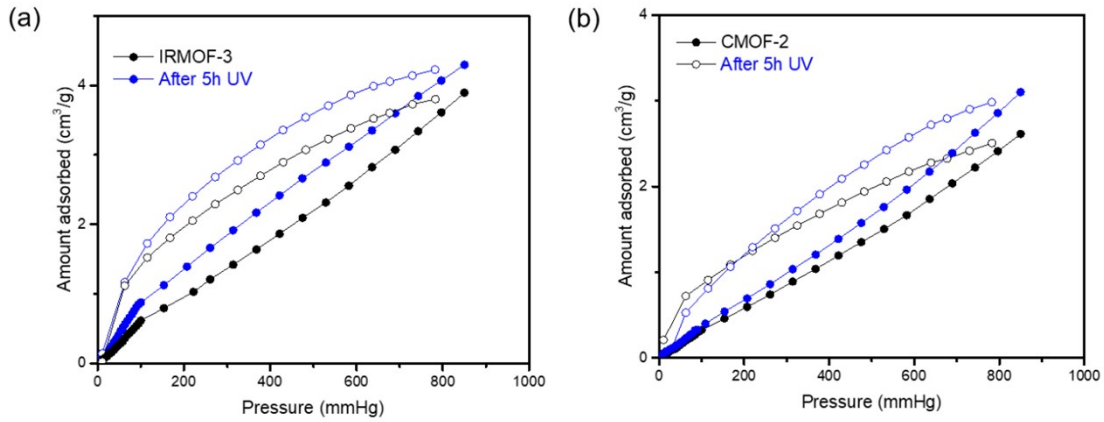

Figure S9. CO_2 adsorption isotherms (at 273 K) of (a) IRMOF-3 and (b) CMOF-2 showing conformational change: right after the first UV irradiation (blue). Results

keeps similar after same time UV irradiation.

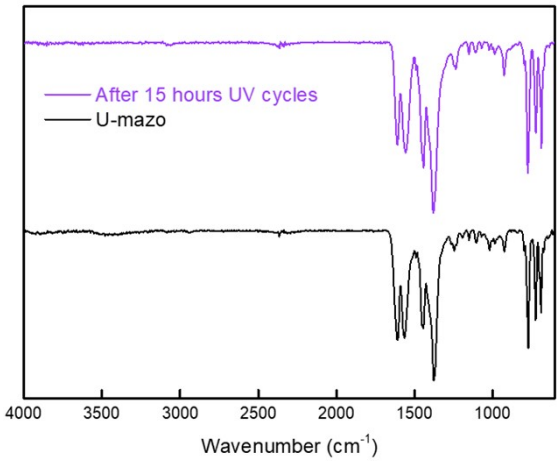

Figure S10. FT-IR spectra of U-mazo and after three cycles of 5 hours UV light irradiation.

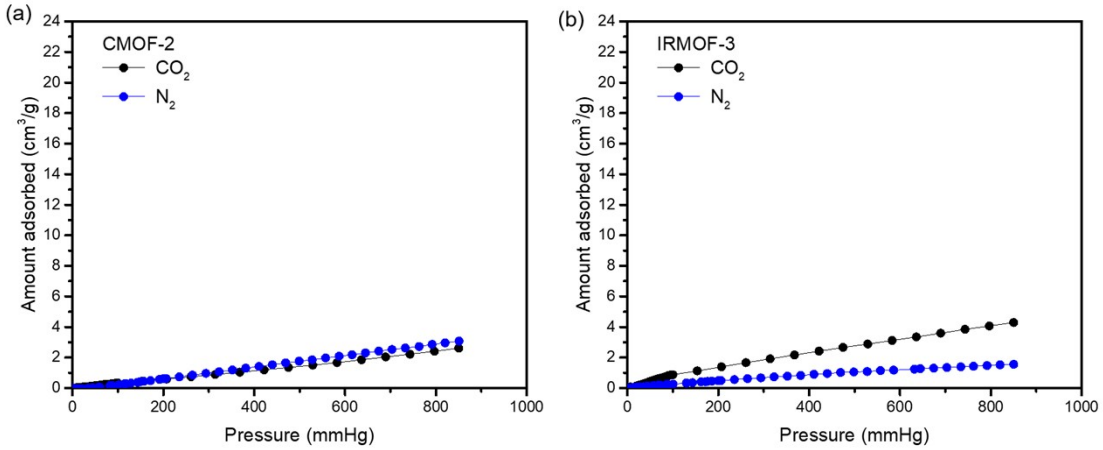

Figure S11. CO_2 and N_2 adsorption isotherms of (a) CMOF-2 and (b) IRMOF-3 at 273 K.

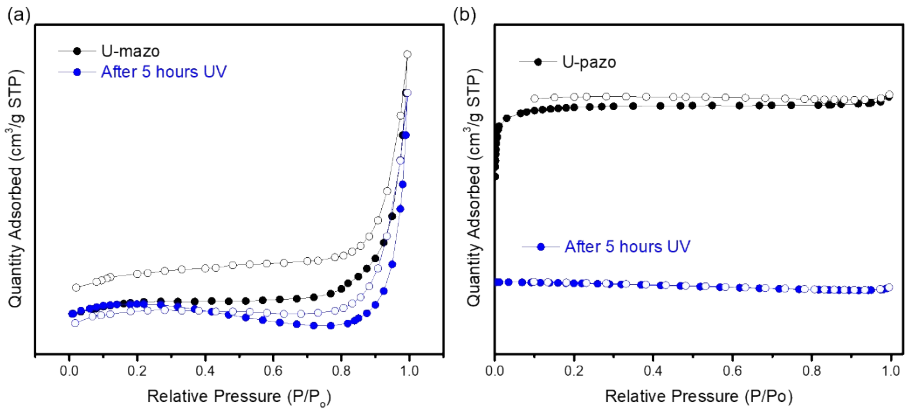

Figure S12. N_2 adsorption isotherms of (a) U-mazo and (b) U-pazo at 77 K and the

results right after the first UV irradiation at 365±10 nm (blue).

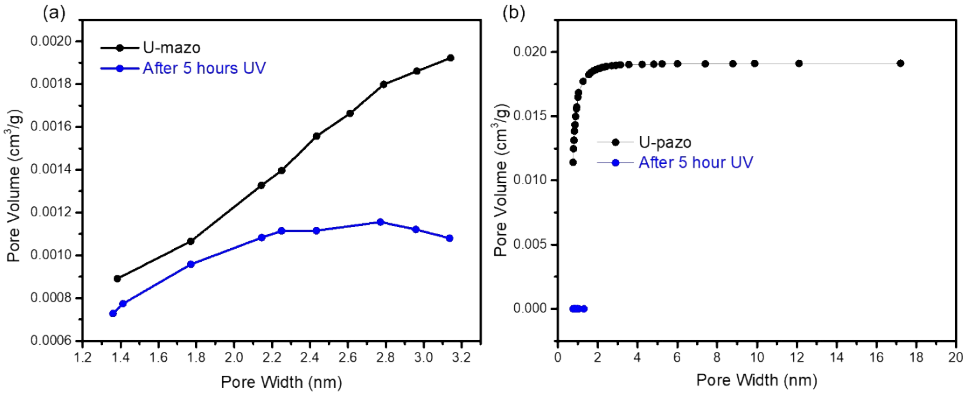

Figure S13. Pore size distribution of U-mazo and U-pazo and the results after UV light irradiation (blue).

Table S1. BET surface area and pore volumes of U-mazo and U-pazo in trans and cis isomers

	BET surface area ($m^2\ g^{-1}$)	Pore volume ($cm^3\ g^{-1}$)
U-mazo (trans)	4.8	0.0264
U-mazo (cis)	3.0	0.0099
U-pazo (trans)	68.8	0.0164
U-pazo (cis)	0.8	0.0015

Table S2. Reported photo switching MOFs

	Switchable moiety	**Incorporation method**	**CO_2 uptake mmol/g**	**Photo triggered release capacity**	**Ref**
PCN-123	AB	Side group	1.0 (295K)	53.9%	[5]
Zn(AzDC)(4,4'-BPE)$_{0.5}$	AB	backbone	1.3 (303K)	42%	[6]
Zn(L)(bpdc)·solvents (1)	DET	backbone	0.9 (298K)	75%	[7]
ECUT-15	AB	backbone	0.3 (298K)	45%	[8]
ZW MOF	pyridinium 4-carboxylate	backbone	0.8 (273 K)	43.2%	[9]
F-azo-MIL-53(Al)	AB	Side group	0.8 (273K, 0.035 P/P_0)	15%	[10]
$Co_2L_2(AzoD)_2$·2DMF	AB	backbone	0.9 (273 K)	21.4%	[11]
Ag/UiO-66-1	AgNCs	guest	1.5 (298 K)	57.7%	[12]
Ag/UiO-66-2			1.1 (298 K)	71.3%	
Ag/UiO-66-3			1.0 (298 K)	80.9%	
PCN-250	AB	backbone	3.8 (298 K)	57.5%	[13]
mPCN-M	AB	backbone	3.4 (298 K)	30.0%	[14]
mPCN-H			3.5 (298 K)	30.7 %	
mPCN-L			4.3 (298 K)	29.4 %	
[Zn2(3,3′-bpeab)(oba)2]·DMF	AB	backbone	1.69 (298 K)	15%	[15]
ECUT-30a	AB and DET		1.3 (273K)	28.6%	[16]
^{Azo}MOF	AB	Side group	19 (195K)	15%	[17]
JUC-62	AB	backbone	2.1 (298 K)	34%	[18]
$Zn_2(bdc)_2(LO)]_n$	DET	backbone	6.1 (195 K)	20%	[19]
Azo-UiO-66	AB	Side group	0.76 (298 K)	33%	[20]
Azo-DMOF-1	AB	Side group	1.8 (298 K)	35%	[21]
T(7.5)/U-azo	AB	Side group	1.8 (273K)	45.6%	[22]

Reference

[1] J. Furthmiiller G. Kresse* *Comput. Mater. Sci.*, 1996, **6**, 15-50.

[2] J. P. Perdew, K. Burke and M. Ernzerhof, *The American Physical Society*, 1996, **77**, 3865-3868.

[3] P. E. Blochl, *Phys Rev B Condens Matter*, 1994, **50**, 17953-17979.

[4] S. Grimme, *Journal of Computational Chemistry*, 2006, **27**, 1787-1799.

[5] J. Park, D. Yuan, K. T. Pham, J. R. Li, A. Yakovenko and H. C. Zhou, *J. Am. Chem. Soc.*, 2012, **134**, 99-102.

[6] R. Lyndon, K. Konstas, B. P. Ladewig, P. D. Southon, P. C. Kepert and M. R. Hill, *Angew. Chem. Int. Ed.*, 2013, **52**, 3695-3698.

[7] F. Luo, C. B. Fan, M. B. Luo, X. L. Wu, Y. Zhu, S. Z. Pu, W. Y. Xu and G. C. Guo, *Angew. Chem. Int. Ed.*, 2014, **53**, 9298-9301.

[8] L. Gong Le, X. F. Feng and F. Luo, *Inorg. Chem.*, 2015, **54**, 11587-11589.

[9] W. An, D. Aulakh, X. Zhang, W. Verdegaal, K. R. Dunbar and M. Wriedt, *Chem. Mater.*, 2016, **28**, 7825-7832.

[10] S. Castellanos, A. Goulet-Hanssens, F. Zhao, A. Dikhtiarenko, A. Pustovarenko, S. Hecht, J. Gascon, F. Kapteijn and D. Bleger, *Chemistry*, 2016, **22**, 746-752.

[11] L. Dang, X. Zhang, L. Zhang, J. Li, F. Luo and X. Feng, J. Coord. Chem., 2016, **69**, 1179-1187.

[12] H. Li, M. R. Hill, C. Doblin, S. Lim, A. J. Hill and P. Falcaro, *Adv. Funct. Mater.*, 2016, **26**, 4815-4821.

[13] H. Li, M. R. Martinez, Z. Perry, H. C. Zhou, P. Falcaro, C. Doblin, S. Lim, A. J. Hill, B. Halstead and M. R. Hill, *Chemistry*, 2016, **22**, 11176-11179.

[14] H. Li, M. Munir Sadiq, K. Suzuki, C. Doblin, S. Lim, P. Falcaro, A. J. Hill and M. R. Hill, *J. Mater. Chem. A*, 2016, **4**, 18757-18762.

[15] W. C. Song, X. Z. Cui, Z. Y. Liu, E. C. Yang and X. J. Zhao, *Sci. Rep.*, 2016, **6**, 34870.

[16] C. B. Fan, Z. Q. Liu, L. L. Gong, A. M. Zheng, L. Zhang, C. S. Yan, H. Q. Wu, X. F. Feng and F. Luo, *Chem. Commun.*, 2017, **53**, 763-766.

[17] H. Huang, H. Sato and T. Aida, *J. Am. Chem. Soc.*, 2017, **139**, 8784-8787.

[18] N. Prasetya and B. P. Ladewig, *Sci. Rep.*, 2017, **7**, 13355.

[19] Y. Zheng, H. Sato, P. Wu, H. J. Jeon, R. Matsuda and S. Kitagawa, *Nat. Commun.*, 2017, **8**, 100.

[20] N. Prasetya, B. C. Donose and B. P. Ladewig, *J. Mater. Chem. A*, 2018, **6**, 16390-16402.

[21] N. Prasetya and B. P. Ladewig, *ACS. Appl. Mater. Interfaces*, 2018, **10**, 34291-34301.

[22] Y. Jiang, P. Tan, S. C. Qi, X. Q. Liu, J. H. Yan, F. Fan and L. B. Sun, *Angew. Chem. Int. Ed.*, 2019, **58**, 6600-6604.